DOI: 10.1002/anie.201403145

Chiral Separation

Functionalized Graphene as a Gatekeeper for Chiral Molecules: An Alternative Concept for Chiral Separation**

Andreas W. Hauser, Narbe Mardirossian, Julien A. Panetier, Martin Head-Gordon, Alexis T. Bell, and Peter Schwerdtfeger**

Abstract: *We propose a new method of chiral separation using functionalized nanoporous graphene as an example. Computational simulations based on density functional theory show that the attachment of a suitable chiral "bouncer" molecule to the pore rim prevents the passage of the undesired enantiomer while letting its mirror image through.*

Enantiomeric forms of a drug molecule may differ in potency, toxicity, and their effect on biological systems. Modern drug research and development requires that enantiomers of all bioactive molecules be separated and tested.[1,2] Enantioselective synthesis would be the ideal way to obtain either left- or right-handed drug molecules, but in most cases this approach is impractical and too expensive. Hence, the separation of intermediate forms or final products from racemic mixtures is often required. Common separation methods are gas chromatography (GC), high-performance liquid chromatography (HPLC), and capillary electrophoresis (CE).[1–3]

Despite recent efforts focusing on physical separation methods, such as photoinduced drift in a gas buffer[4] and separation in microfluidic systems,[5–8] all common and industrially relevant techniques are based on an enantioselective interaction between the drug enantiomers and a chiral selector. Chromatography-based methods, particularly HPLC, have dominated the separation of enantiomers for decades due to their preparative-scale capabilities, but they require expensive equipment, consume large amounts of buffer solutions, and are slow and labor-intensive. Capillary electrophoresis, on the other hand, is less laborious and has a reduced environmental impact, but is comparatively limited in terms of throughput.[9] In all approaches mentioned above, the separation is based on a summation of a series of molecular interactions which occur during the propagation of a drug molecule through some material. The macroscopic result is either a difference in retention time (GC, HPLC) or mobility (CE) for different enantiomers.

Clearly, it would be far more effective if every molecular recognition event, e.g., the identification of a left- or right-handed drug molecule, contributed to the macroscopic separation in terms of a yes-or-no decision. Herein we show that a suitably functionalized, porous sheet of graphene is capable of doing exactly that. We note that a realization of the proposed concept is not restricted to graphene templates, but might, for example, also be accomplished using two-dimensional, porous metal–organic frameworks (MOFs).[10,11]

Free-standing sheets of graphene, discovered in 2004,[12] can be seen as ultimate membranes for molecular sieving due to their single-atom thickness.[13] However, their impermeability to particles as small as helium atoms[14] requires that pores be created by various techniques.[15–20]

Symmetry dictates chiral ineffectiveness for any kind of perfect two-dimensional membrane. This is easily demonstrated by shadow playing, where the left and right hand can be positioned so that they cast the same shadow onto a screen. Regardless of how we shape a cutout or "pore" in a membrane, either both enantiomers will fit through it or neither of them will. This case has to be distinguished from chiral recognition on molecular surfaces, where an additional distinction comes from the specification of "outside" and "inside", that is, the direction of the surface vector. This is demonstrated in Figure 1, where we use the common model of a three-point interaction between a surface and a molecule to underline that molecule B cannot dock onto the matching receptors unless we allow it to reach them from "behind" or "inside". However, both molecules would encounter the same barrier when propagating through a similarly in-plane functionalized pore. The reaction pathways for the two cases would be mirror images, but without physical consequences.

Therefore, chiral recognition has to be introduced to the pore by appropriate out-of-plane functionalization. This is achieved by the attachment of a suitable chiral molecule to the rim of the pore. We refer to this particular molecule as the "bouncer" (or gatekeeper) since its duty is to allow only one type of enantiomer to propagate through the pore while preventing its mirror image from entering. The key concept of our approach is to transfer a small difference in the geometry of a dimer complex formed by the "bouncer" and a penetrating molecule into a big difference for the energetic barrier the latter has to overcome in order to pass through the pore. This idea is illustrated in Figure 2, where we pick 1-aminoethanol

[*] A. W. Hauser, A. T. Bell
Department of Chemical and Biomolecular Engineering
University of California, Berkeley, CA 94720-1462 (USA)
E-mail: andreas.w.hauser@gmail.com
N. Mardirossian, J. A. Panetier, M. Head-Gordon
Department of Chemistry
University of California, Berkeley, CA 94720-1462 (USA)
P. Schwerdtfeger
Centre for Theoretical Chemistry and Physics (CTCP)
The New Zealand Institute for Advanced Study (NZIAS)
Massey University
Bob Tindall Building, 0632 Auckland (New Zealand)
E-mail: peter.schwerdtfeger@gmail.com

[**] A.W.H. thanks Joseph Gomes and Felix Fischer for helpful discussions. Calculations were performed on a cluster provided by the UC Berkeley College of Chemistry through the National Science Foundation (NSF) (Grant CHE-1048789).

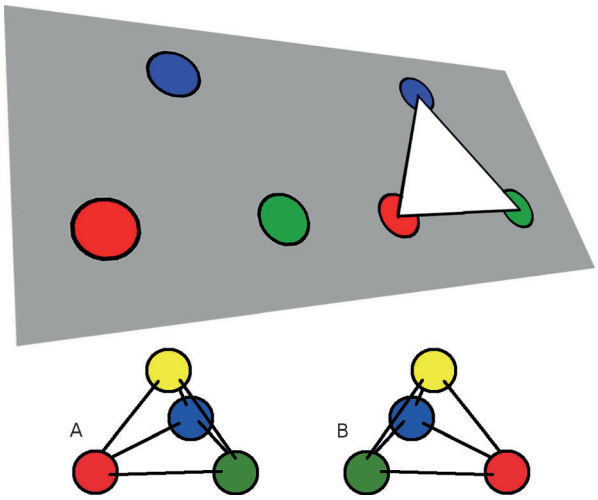

Figure 1. Three-point interaction of a chiral object with either an intact surface or a hole in a surface. We assume matching colors as energetically preferred arrangements. Chiral recognition is granted for a surface (left), but lost in the case of a pore (right). Object A will enter with the red-green-blue face first, while object B prefers to enter with the yellow tip in the head position, but both enantiomers fit equally well through the hole.

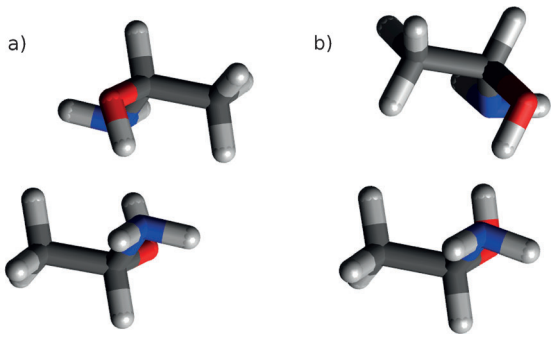

Figure 2. 1-Aminoethanol dimer complexes, stabilized by hydrogen bonds between the amine and hydroxy groups. Complex (a) is formed by molecules of the opposite chirality, while complex b) contains two molecules of the same chirality. In the latter case, the minimum-energy structure is less compact due to repelling methyl groups.

as a small organic chiral representative and optimize the structure of the dimer, which contains two molecules of either the same or opposite chirality. Electronic energies are obtained from density functional theory. The cc-pVDZ basis set[21] and the B97-D functional of Grimme[22] are used for unconstrained optimizations, transition-state searches, and frequency calculations. Counterpoise-corrected single-point energies at converged geometries are evaluated with the aug-cc-pVDZ basis.[23,24] All calculations are performed with a developer version of the Q-Chem program package.[25]

The binding energies of the two dimer complexes differ by only 1.7 kcal mol^{-1}. This difference is too small for the suggested purpose of chiral separation. However, the relaxed geometries of the two dimers show a significant deviation. The same-pair complex (b) is less compact than the mixed-pair complex (a) due to unfavorable positioning of the two methyl groups. The distance between the chiral centers of the two molecules is 0.17 Å larger for the same-pair complex. This small difference in size is now easily converted into a desired big difference for the transmission barrier: we attach one molecule as a permanent functionalization to the rim of a graphene pore and choose the pore size so that it is big enough for the mixed-pair complex to fit through, but too small for the same-pair complex. Formation of the latter by the interaction of an undesired molecule with the "bouncer" at the pore entrance requires more space and is hindered by Pauli repulsion. The methyl group of the free molecule is repelled by the upper rim, leading to a much higher transmission barrier. The desired enantiomer, on the other hand, is able to form a dimer complex which is small enough to allow propagation. The corresponding transition states are illustrated in Figure 3. Our findings are closely related to recent

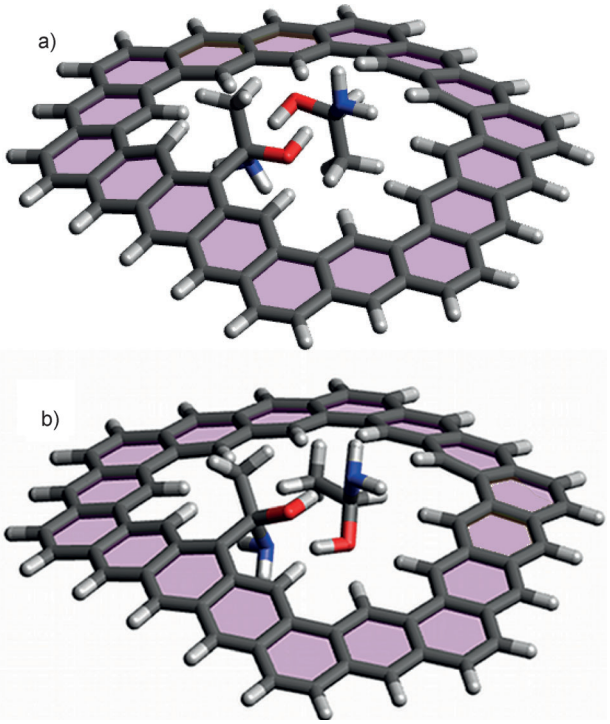

Figure 3. Rate-determining transition states formed by the interaction of a "bouncer" 1-aminoethanol molecule attached to the pore rim with a free 1-aminoethanol molecule of opposite (a) or same (b) chirality, simulated in a finite pore model consisting of 17 rings. In case (b), the structure of the dimer complex, which is dictated by the hydrogen bonds between amine and hydroxy groups, is slightly too large for the pore.

studies on adsorption-based (and therefore stochastic) separation in homochiral MOFs.[26,27]

We identified a trapezoid-shaped hole as a suitable model pore, which is formally obtained by removing five rings from a perfect graphene sheet. Due to computational limitations, we chose a finite pore model which consists of the 17 surrounding carbon rings passivated with hydrogen atoms. In the first step, we attach the "bouncer" molecule to the pore

rim by replacing one of the inner passivating hydrogen atoms and allow the whole structure to relax. Next, we add another 1-aminoethanol molecule of either the same or opposite chirality to the system and calculate the reaction pathway for its transmission through the pore. The first-order saddle points are localized by a combination of the freezing string method[28] and a hessian mode following approach.[29] IRC calculations and subsequent geometry optimizations are used to confirm the minima linked by each transition state. Having identified the most stable intermediates and transition states, we calculate the Gibbs free energies within the harmonic oscillator approach from DFT frequencies, including zero-point energy corrections. To account for hindered rotations in the evaluation of numerical frequencies, we apply an ad hoc correction[30] which suggests a continuous interpolation between vibrational (S_v) and rotational (S_R) contributions to the entropy according to the Equation (1) with the weighting function given in Equation (2) and a cutoff value of $\omega_0 = 100\ cm^{-1}$. Our results are summarized in Table 1.

Table 1: DFT electronic energies and Gibbs free energies (at normal conditions, in kcal mol^{-1}) for the adsorption and the transmission of a 1-aminoethanol molecule through a chirally functionalized graphene pore. The descriptions "opposite" and "same" refer to the chirality of the free gas molecule with respect to the "bouncer" molecule.

Geometry	ΔE	ΔG[a]	
desorbed mol.	0.00	0.00	[0.00]
opposite enantiomers:			
left minimum	−21.37	−3.90	[−4.44]
1st transition state	−8.34	11.20	[11.90]
intermediate	−10.95	8.24	[8.39]
2nd transition state	−10.43	8.92	[9.38]
right minimum	−18.00	−0.99	[−1.67]
Identical enantiomers:			
left minimum	−20.26	−3.63	[−4.45]
1st transition state	−8.99	9.07	[9.05]
intermediate	−9.44	8.30	[8.14]
2nd transition state	−0.27	19.66	[20.45]
right minimum	−21.14	−3.97	[−4.68]

[a] ΔG values are corrected for hindered rotations. Uncorrected values are given in brackets.

$$S = w(\omega)S_v + [1-w(\omega)]S_R, \quad (1)$$

$$w(\omega) = \frac{1}{1+(\omega_0/\omega)^4} \quad (2)$$

Schematic reaction pathways including Gibbs free energies and corresponding geometries are shown in Figure 4. Due to the strong hydrogen bonds, we obtain DFT adsorption energies between −18.0 and −21.4 kcal mol^{-1}. In both pathways even the transition state energies remain below zero. However, after thermodynamic correction at 25 °C and 1 atm, all apparent transition state barriers become positive. The rate-determining highest-energy transition states in each reaction pathway are slightly reduced by the correction for hindered rotations. We find ΔG values of 11.2 and 19.7 kcal mol^{-1} for a molecule of opposite and same chirality with respect to the "bouncer" molecule, respectively.

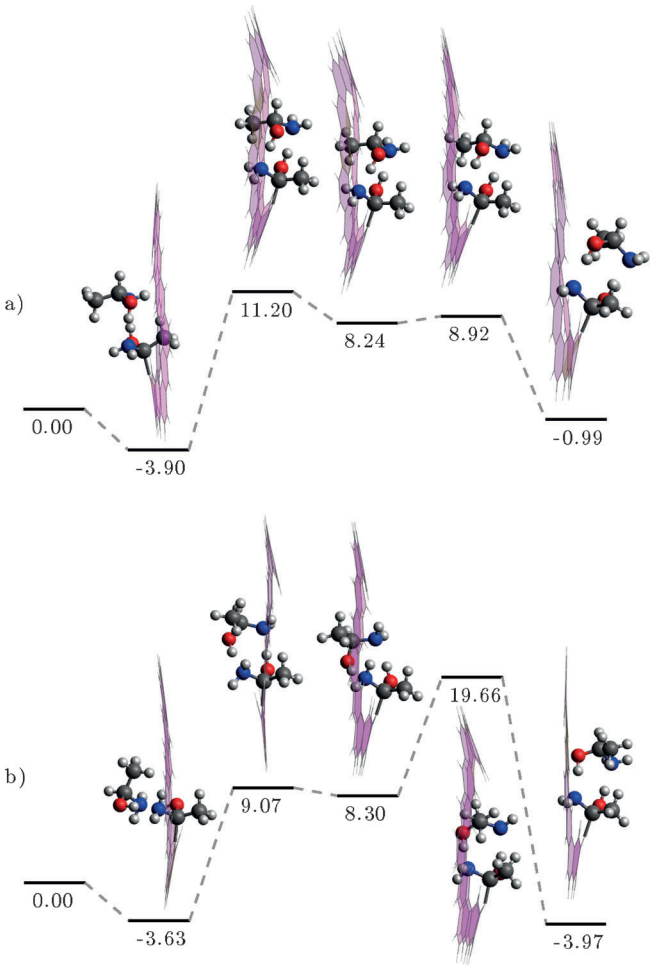

Figure 4. Schematic reaction pathways for the propagation of a 1-aminoethanol molecule through a chirally functionalized graphene pore. Path (a) describes the interaction between a '"bouncer"' and free molecule of opposite chirality, while path (b) describes that of same chirality. Gibbs free energies are given in kcal mol^{-1}.

The propagation of a gas molecule through the pore can be considered a "chemical reaction", where the reactants are the pore and the gas molecule on the left side, and the products are the pore and the molecule on the right side. Assuming that the activated complex is in equilibrium with the reactants, we can apply transition state theory to obtain a formula for the rate constant of the propagation [Eq. (3)][32,33], where k_b is the Boltzmann constant, h is the Planck constant, T is the temperature, and ΔG is the difference of Gibbs free energies between the highest transition state in each pathway and a fully separated system.

$$k_{prop} = \frac{k_b T}{h} exp\left(-\frac{\Delta G}{k_b T}\right), \quad (3)$$

At room temperature, we obtain a rate constant of $3.8 \times 10^4\ s^{-1}$ for a 1-aminoethanol molecule of opposite chirality with respect to the "bouncer" molecule, whereas the rate constant for the enantiomer of same chirality is only $2.4 \times$

$10^{-2}\,s^{-1}$, yielding a separation ratio of about 1.6×10^{6}. Assuming a highly theoretical membrane that consists only of functionalized pores, we can roughly estimate the macroscopic particle flux for the accepted species as 2.8×10^{-6} mol per square centimeter per second. The large separation ratio also leaves room for a suitable adjustment of process temperature to minimize pore blocking due to adsorption.

To summarize, we propose a novel concept for the separation of enantiomers with chirally functionalized, nanoporous graphene. Chiral recognition is introduced by the permanent attachment of a chiral "bouncer" molecule to the pore rim. Free gas-phase enantiomers form a dimer complex with the "bouncer" molecule during propagation. This dimer complex differs in size, depending on the chirality of the free molecule with respect to the chirality of the "bouncer" molecule. With a properly chosen pore size, one enantiomer is able to pass through, while the other is not. In contrast to conventional separation procedures, this new technique separates different enantiomers in a single molecular event. Its effectiveness has been demonstrated for nanoporous graphene, but realization of the separation mechanism is not limited to this particular type of membrane. The underlying idea to exploit the size differences of dimer complexes for the follow-up separation by means of Pauli repulsion might be introduced to metal-organic framework chemistry through the careful selection of chiral or chirally functionalized linkers in two-dimensional structures. We believe that this new concept could become a cheap and highly efficient alternative to current separation methods and hope that our findings stimulate further research in the field of membrane synthesis and functionalization.

Received: March 9, 2014
Published online: July 13, 2014

Keywords: chiral separation · enantiomers · graphene · racemic mixture

[1] J. E. Rekoske, *AIChE J.* **2001**, *47*, 2 – 5.
[2] G. Gübitz, M. G. Schmid, *Mol. Biotechnol.* **2006**, *32*, 159 – 179.
[3] T. J. Ward, B. A. Baker, *Anal. Chem.* **2008**, *80*, 4363 – 4372.
[4] B. Spivak, A. V. Andreev, *Phys. Rev. Lett.* **2009**, *102*, 063004.
[5] M. Kostur, M. Schindler, P. Talkner, P. Hänggi, *Phys. Rev. Lett.* **2006**, *96*, 014502.
[6] R. Eichhorn, *Phys. Rev. Lett.* **2010**, *105*, 034502.
[7] R. Eichhorn, *Chem. Phys.* **2010**, *375*, 568 – 577.
[8] S. Meinhardt, J. Smiatek, R. Eichhorn, F. Schmid, *Phys. Rev. Lett.* **2012**, *108*, 214504.
[9] B. Li, D. T. Haynie, *Encyclopedia of Chemical Processing*, Taylor and Francis, New York **2007**, Chap. 44, pp. 449 – 458.
[10] B. Kesanli, W. Lin, *Coord. Chem. Rev.* **2003**, *246*, 305 – 326.
[11] W. Lin, *MRS Bull.* **2007**, *32*, 544 – 548.
[12] K. S. Novoselov, A. K. Geim, S. V. Morozov, D. Jiang, Y. Zhang, S. V. Dubonos, I. V. Grigorieva, A. A. Firsov, *Science* **2004**, *306*, 666 – 669.
[13] S. Oyama, D. Lee, P. Hacarlioglu, R. Saraf, *J. Membr. Sci.* **2004**, *244*, 45 – 53.
[14] O. Leenaerts, B. Partoens, F. M. Peeters, *Appl. Phys. Lett.* **2008**, *93*, 193107.
[15] M. D. Fischbein, M. Drndic, *Appl. Phys. Lett.* **2008**, *93*, 113107.
[16] P. Kuhn, A. Forget, D. Su, A. Thomas, M. Antonietti, *J. Am. Chem. Soc.* **2008**, *130*, 13333 – 13337.
[17] D. C. Bell, M. C. Lemme, L. A. Stern, J. R. Williams, C. M. Marcus, *Nanotechnology* **2009**, *20*, 455301.
[18] S. Huh, J. Park, Y. S. Kim, K. S. Kim, B. H. Hong, J.-M. Nam, *ACS Nano* **2011**, *5*, 9799 – 9806.
[19] P. Xu, J. Yang, K. Wang, Z. Zhou, P. Shen, *Chin. Sci. Bull.* **2012**, *57*, 2948 – 2955.
[20] S. P. Koenig, L. Wang, J. Pellegrino, J. S. Bunch, *Nat. Nanotechnol.* **2012**, *7*, 728 – 732.
[21] T. H. J. Dunning, *J. Chem. Phys.* **1989**, *90*, 1007 – 1023.
[22] S. Grimme, *J. Comp. Physiol.* **2006**, *27*, 1787 – 1799.
[23] A full counterpoise correction scheme including monomer deformations is applied.
[24] N. Mardirossian, M. Head-Gordon, *J. Chem. Theory Comput.* **2013**, *9*, 4453 – 4461.
[25] Y. Shao, L. F. Molnar, Y. Jung, J. Kussmann, C. Ochsenfeld, S. T. Brown, A. T. B. Gilbert, L. V. Slipchenko, S. V. Levchenko, D. P. O'Neill, R. A. DiStasio, Jr., R. C. Lochan, T. Wang, G. J. O. Beran, N. A. Besley, J. M. Herbert, C. Y. Lin, T. Van Voorhis, S. H. Chien, A. Sodt, R. P. Steele, V. A. Rassolov, P. E. Maslen, P. P. Korambath, R. D. Adamson, B. Austin, J. Baker, E. F. C. Byrd, H. Dachsel, R. J. Doerksen, A. Dreuw, B. D. Dunietz, A. D. Dutoi, T. R. Furlani, S. R. Gwaltney, A. Heyden, S. Hirata, C.-P. Hsu, G. Kedziora, R. Z. Khalliulin, P. Klunzinger, A. M. Lee, M. S. Lee, W. Liang, I. Lotan, N. Nair, B. Peters, E. I. Proynov, P. A. Pieniazek, Y. M. Rhee, J. Ritchie, E. Rosta, C. D. Sherrill, A. C. Simmonett, J. E. Subotnik, H. L. Woodcock III, W. Zhang, A. T. Bell, A. K. Chakraborty, D. M. Chipman, F. J. Keil, A. Warshel, W. J. Hehre, H. F. Schaefer III, J. Kong, A. I. Krylov, P. M. W. Gill, M. Head-Gordon, *Phys. Chem. Chem. Phys.* **2006**, *8*, 3172 – 3191.
[26] X. Bao, L. J. Broadbelt, R. Q. Snurr, *Microporous Mesoporous Mater.* **2012**, *157*, 118 – 123.
[27] X. Bao, R. Q. Snurr, L. J. Broadbelt, *Microporous Mesoporous Mater.* **2013**, *172*, 44 – 50.
[28] A. Behn, P. M. Zimmerman, A. T. Bell, M. Head-Gordon, *J. Chem. Phys.* **2011**, *135*, 224108.
[29] J. Baker, *J. Comput. Chem.* **1986**, *7*, 385 – 395.
[30] S. Grimme, *Chem. Eur. J.* **2012**, *18*, 9955 – 9964.
[31] The identical adsorption energies for both enantiomers onto a perfect graphene sheet indicate balanced surface-residence probabilities. Therefore, we expect essentially unbiased propagation statistics in future dynamical simulations.
[32] S. S. Glasstone, K. Laidler, H. Eyring, *The Theory of Rate Processes*, McGraw-Hill, New York, **1941**.
[33] D. A. McQuarrie, J. D. Simon, *Physical Chemistry: A Molecular Approach*, University Science Books, Sausalito, **1997**.

